Interface focus

J. R. Soc. Interface (2010) **7**, S393–S402
doi:10.1098/rsif.2010.0099.focus
Published online 2 June 2010

Size mapping of electric field-assisted production of polycaprolactone particles

M. Enayati, Z. Ahmad, E. Stride and M. Edirisinghe*

Department of Mechanical Engineering, University College London, Torrington Place, London WC1E 7JE, UK

In this investigation, biodegradable polycaprolactone polymeric particles (300–4500 nm in diameter) were prepared by jetting a solution in an electric field. An extensive study has been carried out to determine how the size and size distribution of the particles generated can be controlled by systematically varying the polymer concentration in solution (and thereby its viscosity and electrical conductivity), and also the selected flow rate (2–50 $\mu l\,min^{-1}$) and applied voltage (0–15 kV) during particle generation. Change in these parameters affects the mode of jetting, and within the stable cone-jet mode window, an increase in the applied voltage (approx. 15 kV) resulted in a reduction in particle size and this was more pronounced at high flow rates (such as; 30, 40 and 50 $\mu l\,min^{-1}$) in the same region. The carrier particles were more polydisperse at the peripheral regions of the stable cone-jet mode, as defined in the applied voltage-flow rate parametric map. The effect of loading a drug on the particle size, size distribution and encapsulation efficiency was also studied. Release from drug-loaded particles was investigated using UV spectrophotometry over 45 days. This work demonstrates a powerful method of generating drug-loaded polymeric particles, with the ability to control size and polydispersivity, which has great potential in several categories of biotechnology requiring carrier particles, such as drug delivery and gene therapy.

Keywords: size; mapping; polymer; polycaprolactone; jetting

1. INTRODUCTION

There are numerous drug-delivery systems and the goal of most of these is to deliver medications intact to specific targets in the body through a medium that can control the administration of therapy by means of either a physiological or chemical trigger (Song *et al.* 1998; Calvo *et al.* 2001; Kaul & Amiji 2005). One of the most important characteristics to achieve this goal is particle size (Panyam & Labhasetwar 2003), which has a significant effect upon the *in vivo* behaviour such as circulation time, extravasation, targeting, immunogenicity, internalization, intracellular trafficking, degradation, flow properties, clearance and uptake mechanisms (Mitragotri & Lahann 2009). For instance, micrometre-sized particles are important in passive drug targeting such as pulmonary drug delivery. They are suitable for incorporation into aerosols which have potential uses for inhalation devices in the treatment of asthma (Edwards *et al.* 1997; Musante *et al.* 2002; Chowdary & Rao 2004). Nanometre-sized particles also have certain unique applications in drug delivery (Monsky *et al.* 1999) in that they can penetrate small capillaries, allowing enhanced accumulation of nanoparticles at delivered target sites. They are also used in passive targeting of tumour tissue through enhanced permeation and retention effects (Oyewumi & Mumper 2003; Stroh *et al.* 2005). Thus, particle diameter dictates their transport and adhesion in blood vessels, airways or the gastro-intestinal tract and can also influence the clearance mechanisms of the particles from the body (Lanza *et al.* 2002).

Biodegradable polymers are the preferred choice of materials for fabricating particles as drug-delivery carriers. They are effective in enhancing drug-targeting specificity, lowering systemic drug toxicity, improving treatment absorption rates and providing protection for pharmaceuticals against biochemical degradation (Reed & Gilding 1981). Polyesters (such as poly(glycolic acid) (PGA), poly(lactic acid) (PLA), poly (lactic-co-glycolic acid) (PLGA) and poly (ε-caprolactone) (PCL)) are considered the most suitable types of biodegradable polymer as they demonstrate low immunogenicity and toxicity. Hence, such polymeric vehicles demonstrate greater biocompatibility and their physicochemical and mechanical properties can also be tailored via selection of polymer molecular weight, copolymerization and functionalization (Shive & Anderson 1997). The advantages of using PCL for preparing therapeutic delivery devices include: high permeability to small drug molecules; failure to generate an acidic environment during degradation (as is the case with polylactides and

*Author for correspondence (m.edirisinghe@ucl.ac.uk).

One contribution to a Theme Supplement 'Scaling the heights—challenges in medical materials: an issue in honour of William Bonfield, Part I. Particles and drug delivery'.

Received 22 February 2010
Accepted 12 May 2010

glycolides); an exceptional ability to form blends with other polymers; and slow degradation rate of the PCL homopolymers compared with PLGA which makes it more suitable for long-term delivery systems, i.e. for periods of more than one year (Aberturas *et al.* 2002).

Numerous methods have been used to fabricate micro- and nanoparticles of various sizes, including emulsion polymerization, microfabrication, self-assembly and electric jetting (Mitragotri & Lahann 2009). Among these methods, those using jetting processes have recently attracted the attention of many researchers for generating vehicles for delivering drugs because of their capability for generating monodisperse particles with a narrow size distribution and also depositing small structures in a controlled fashion (Xie *et al.* 2006; Wang & Stark 2010). In this technique, a liquid (which is composed of polymer and the active agent, e.g. drug, hormone or even cells) is perfused through an electrified capillary. For appropriate values of both the applied electric potential and flow rate, the meniscus at the needle exit develops an almost conical shape and a very thin capillary jet is ejected from its vertex. Depending on the specific processing parameters (e.g. properties and concentration of solution, flow rate and applied voltage), this jet breaks up and can be used to produce micro- and nano-scale polymeric particles at the ambient temperature and pressure (Hartman *et al.* 1999). Active agents can be incorporated into the processing solutions which are then encapsulated (Wu *et al.* 2009).

A systematic investigation of the effects of several key processing parameters specifically: voltage, flow rate, solution properties (such as viscosity and electric conductivity), polymer concentration and drug loading, on the modes of electrospraying processing and on the size/size distribution of the particles produced was carried out in this study. The *in vitro* release profile of β-oestradiol-loaded PCL particles was also studied using UV spectrophotometry. Once the optimal conditions have been mapped, the hormone can be replaced by another material or agent suitable for a host of other biotechnology applications.

2. MATERIAL AND METHODS

2.1. Materials

Polycaprolactone ($M_w = 14\,000$ kDa), dimethylacetamide (DMAC, 99%), β-oestradiol and ethanol (99%) were purchased from Sigma–Aldrich (Poole, UK).

2.2. Methods

2.2.1. Solution preparation. Appropriate quantities of PCL were dissolved in DMAC. The weight ratios of the polymer to the solvent were as follows: (PCL : DMAC) 2 : 98, 5 : 95 and 10 : 90. The polymeric solutions were stirred mechanically at the ambient temperature (25°C) to ensure all the polymer had completely dissolved (15 min). β-Oestradiol of 15 wt% was also added to the individual solutions to investigate the effect of drug loading on the characteristics of the generated particles and also to investigate the release profile.

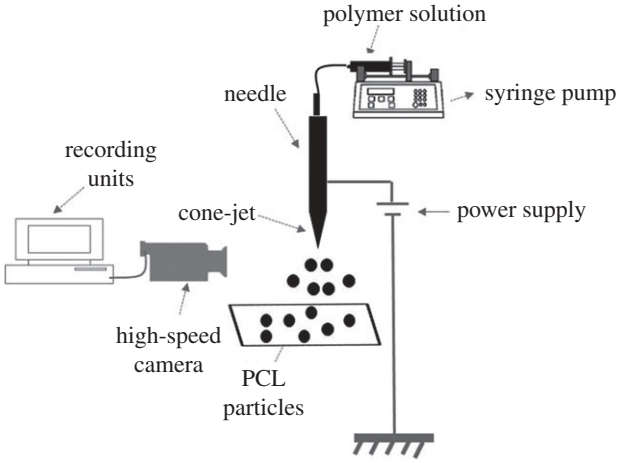

Figure 1. Schematic of the experimental apparatus used for PCL particle production.

2.2.2. Properties of the solutions. The density, viscosity, surface tension and electrical conductivity of the solutions was measured. Densities were calculated using a standard 25 ml density bottle (VWR International, UK) using a high precision scale (six decimal places), and the mean value from five density readings was recorded. Surface tension was measured using a Kruss Tensiometer (Standard Wilhelmy's plate method). The viscosity of the polymer solutions was determined using a U-tube viscometer (BS/U type). Electrical conductivity was estimated using a HI-8733 Hanna Instruments conductivity probe. All the equipment used was initially calibrated using ethanol reference data at the ambient temperature. Ethanol was used as the reference solvent as there are ample data on this and it is a common solvent used to calibrate the equipment used in this work.

2.2.3 Particle production. Figure 1 shows a schematic of the experimental set-up. Temperature and relative humidity were maintained at 23°C and 42 per cent, respectively. PCL solutions were drawn into a 5 ml plastic syringe and placed in a high-precision Harvard syringe pump to control the liquid flow rate. The syringe was connected to a stainless steel needle with an internal diameter of 600 μm. A high-voltage power supply (Glassman Europe Ltd., Tadley, UK) with a capacity to deliver 30 kV was coupled to the stainless steel needle. The flowing polymeric solutions were thus subjected to controlled electric fields, the strength of which were controlled by varying the applied voltage. Voltages from 0 to 18 kV were applied to establish the modes of jetting of the solutions with different viscosities. A high-speed camera was used to observe these modes and the jet/jet-break-up process. At selected flow rates, the stable cone-jet mode was achieved and the processing window, as a function of the applied voltage was obtained (Cloupeau & Prunet-Foch 1990). This mode can generate near-monodisperse, fine droplets. Thus, the relationship between the applied voltage and flow rate and the parametric space for different solutions was established at different spraying modes. All samples were collected

at a working distance of 20 mm below the needle exit on glass microscope slides coated with a thin film of ethanol to avoid coagulation of the particles during formation and collecting. Ethanol was selected as the collection solvent as it is volatile and PCL is insoluble in this solvent. It is also used in numerous biomedical investigations and it evaporates rapidly after particles have been collected (Enayati *et al.* 2010). It must be noted that the porosity and crystallinity of the particles can depend on drying conditions (Valo *et al.* 2009). However in this work microscopical observations did not show significant changes in surface porosity, and the crystallinity was not investigated.

Experimental set-ups, similar to the one used in these studies, can be used in the preparation of biomedical structures for many applications. The needle geometries can be altered simply to accommodate multi-layered morphologies (Ahmad *et al.* 2008), which is another area in the delivery of drugs using smart release mechanisms. The influence of polarity on the jetting process and resultant particles is another area which can be researched (Borra *et al.* 1999), however the more significant factors controlling particle size are the flow-rates and applied voltage (Enayati *et al.* 2009).

2.2.4. Characterization of particles. The morphology and structure of the particles were determined using optical (Nikon eclipse ME600 optical microscope) and scanning electron microscopy (JEOL JSM-6301F field emission, SEM). Samples analysed using SEM were sputter-coated with gold for 60 s prior to examination and analysis was conducted in the acceleration voltage range of 5–10 kV. The diameter of the generated particles was measured using standard SEM images coupled to the UTHSCSA imaging tool program (Image Tool v. 2, University of Texas, USA). This software operates using Borland's C++ programming environment (v.5.0.2) and the mean size of particles was calculated via direct link-up analysis to SEM imaging and magnification.

2.2.5. In vitro *release study. In vitro* release profiles were monitored using an ultraviolet spectrophotometric method (UV-2401PC spectrophotometer, Shimadzu, Japan). The hormone-loaded particles were collected at a working distance of 20 mm below the device exit directly into glass vials containing 50 per cent simulated body fluid (SBF), which has ion concentrations approximately equivalent to that of human blood plasma, and was buffered at pH 7.4. The remaining solution (50%) comprised ethanol, and the time allocated for particle collection was 600 s. SBF : ethanol (50 : 50 v/v) was chosen as the release medium because of the low solubility of β-oestradiol in water or buffered solutions. It is important that the solubility of β-oestradiol is high enough in the release medium, so that it would be the rate of drug release owing to polymer degradation and release that was measured, not the rate of β-oestradiol solubility. The β-oestradiol calibration curve was obtained by dissolving the drug in the SBF : ethanol (50 : 50 v/v) mixture after checking that the presence of ethanol up to 50 per cent modified neither the specific extinction nor the wavelength at which the maximum in UV absorbance appears. All samples were collected in 10 ml of release medium and maintained at 37°C. As this method of particle fabrication involves solvent evaporation, the vast majority of the solvent is lost between the medium jet and the collection stage. The remainder of the solvent is displaced from the particles via phase separation after immersion precipitation. At appropriate time intervals, selected samples were centrifuged at 4300 r.p.m. for 45 min. The supernatant was taken and replaced with an equal amount of fresh release medium. Then the amount of β-oestradiol in the collected supernatant was measured in the UV spectrophotometer at a wavelength of 280 nm. Four replicates were carried out for each release test. Control samples without β-oestradiol were also monitored so that any contributions to the measured absorbance from the polymer could be evaluated.

The amount of unencapsulated drug in the supernatant was measured to determine the encapsulation efficiency (EE). The generated particles were centrifuged at 4300 r.p.m. subsequent to the particle collection. The supernatant was drawn out carefully and the concentration of β-oestradiol in the supernatant was measured using UV spectrophotometry. The EE was expressed as the mass ratio between the amount of β-oestradiol incorporated in the particles and that which was used in the particle preparation.

3. RESULTS AND DISCUSSION

3.1. Characteristics of the solutions

The electric field-assisted process of producing the particles is governed by the physical properties of the solutions (such as surface tension, viscosity, density and electrical conductivity), and also on the processing parameters (flow rate and applied voltage). A combination of these variables determines the different jetting modes (Cloupeau & Prunet-Foch 1990). The measured properties of the polymer solutions used are shown in table 1. The electrical conductivity of the solutions decreased more than four times as the concentration of the polymer increased up to 10 wt% from 2 wt% because of the insulating nature of PCL. Polymer solutions that were further mixed with β-oestradiol demonstrated a slight increase in their electrical conductivities when compared with their parent solutions, suggesting that β-oestradiol causes an increase in the electrical conductivity, while PCL reduces the electrical conductivity. The density and surface tension of the solutions did not change significantly between samples with different polymer concentrations but, as expected, the viscosity increased significantly as a function of polymer concentration.

3.2. Jetting modes of the polymeric solutions

The geometrical features of the jet and the various types encountered as a function of the operating parameters have been classified previously, e.g. by

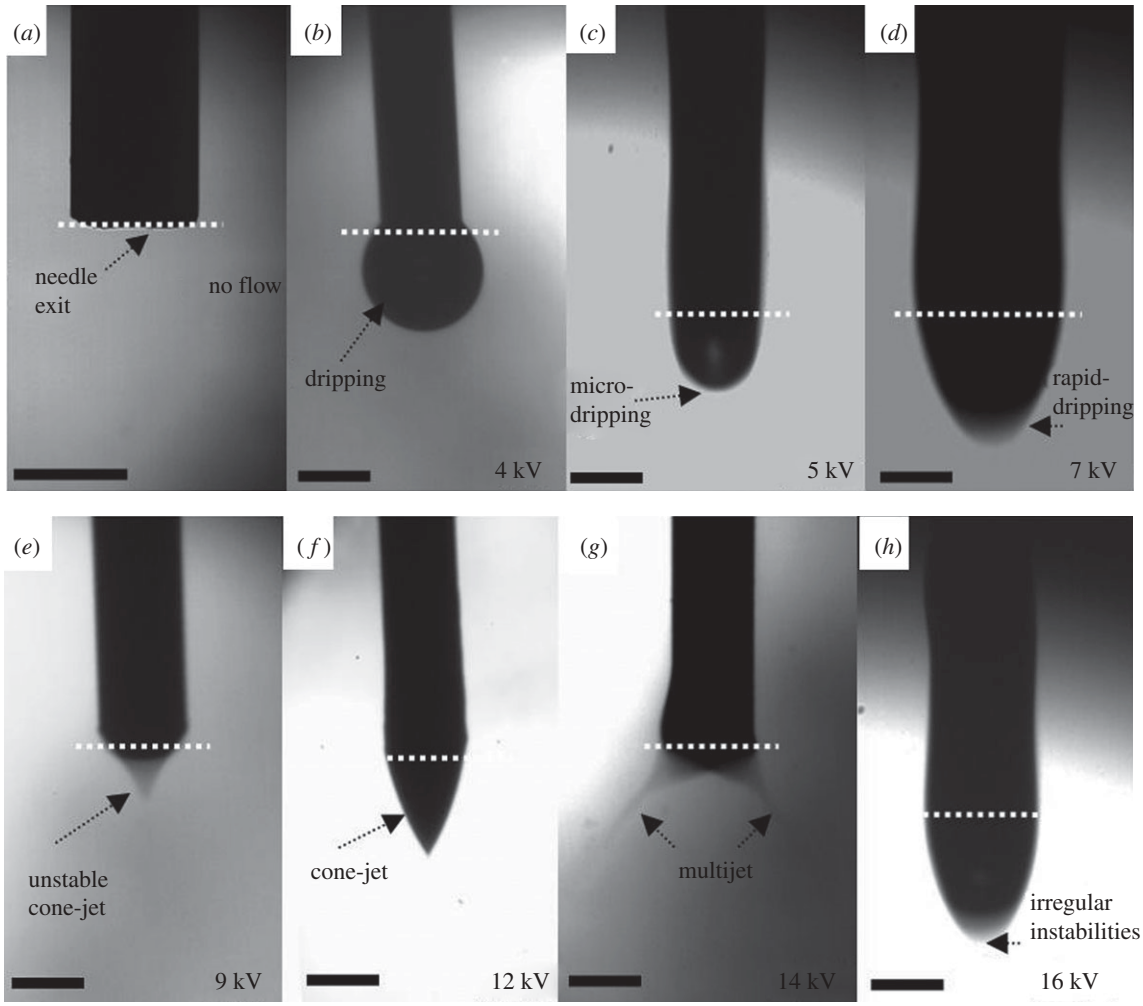

Figure 2. Flow of 5 wt% PCL solution under an electric field showing, with flow rate set at 10 μl min^{-1}, (*a*) no flow, (*b*) dripping mode, (*c*) microdripping mode, (*d*) rapid dripping mode, (*e*) unstable cone-jet mode, (*f*) stable cone-jet mode, (*g*) multi-jet mode, and (*h*) irregular instabilies mode. Scale bars, 600 μm.

Table 1. Properties of the solutions and the solvent used in this study.

sample	density (kg m^{-3})	viscosity (mPa s)	surface tension (mN m^{-1})	electrical conductivity (μS m^{-1})
DMAC	940	2.0	29	5.6
PCL : DMAC 2 : 98	946	2.6	29	3.4
PCL : DMAC 5 : 95	951	4.6	29	1.8
PCL : DMAC 10 : 90	958	11.1	32	0.8
PCL : DMAC 2:98 + 15% ET	947	2.6	29	4.1
PCL : DMAC 5:95 + 15% ET	951	4.6	29	2.5
PCL : DMAC 10 : 90+15% ET	958	11.2	32	1.1

Jaworek & Krupa (1999). These include dripping, microdripping, rapid microdripping, unstable cone-jet, stable cone-jet, multijet and irregular instability modes as shown in figure 2. The cone-jet is the most stable and the most used mode, as it generates a near-uniform particle size distribution (Cloupeau & Prunet-Foch 1990). In our study, the 'dripping mode' (0–4 kV) did not differ significantly from usual dripping under electrically neutral conditions. The drops took the shape of regular spheres detaching from the capillary as the gravity force and the electric force overcame the surface tension forces (figure 2*b*). The increase in the voltage caused a transition to 'cone-jet mode' (9.5–12.5 kV; figure 2*f*), which results as a balance of liquid pressure, liquid surface tension, gravity, electric stresses at the liquid surface, the liquid inertia and the liquid viscosity (Hartman *et al.* 2000). By further increasing the voltage, the 'multijet modes' (13–15 kV) evolved. The multijet mode ceases on further increments to the applied voltage. When irregular instabilities are encountered, one possible form the jet can take is shown in figure 2*h*, where intermittent droplet formation occurs. Compared with unstable jetting (figure 2*d*), although the images may look similar,

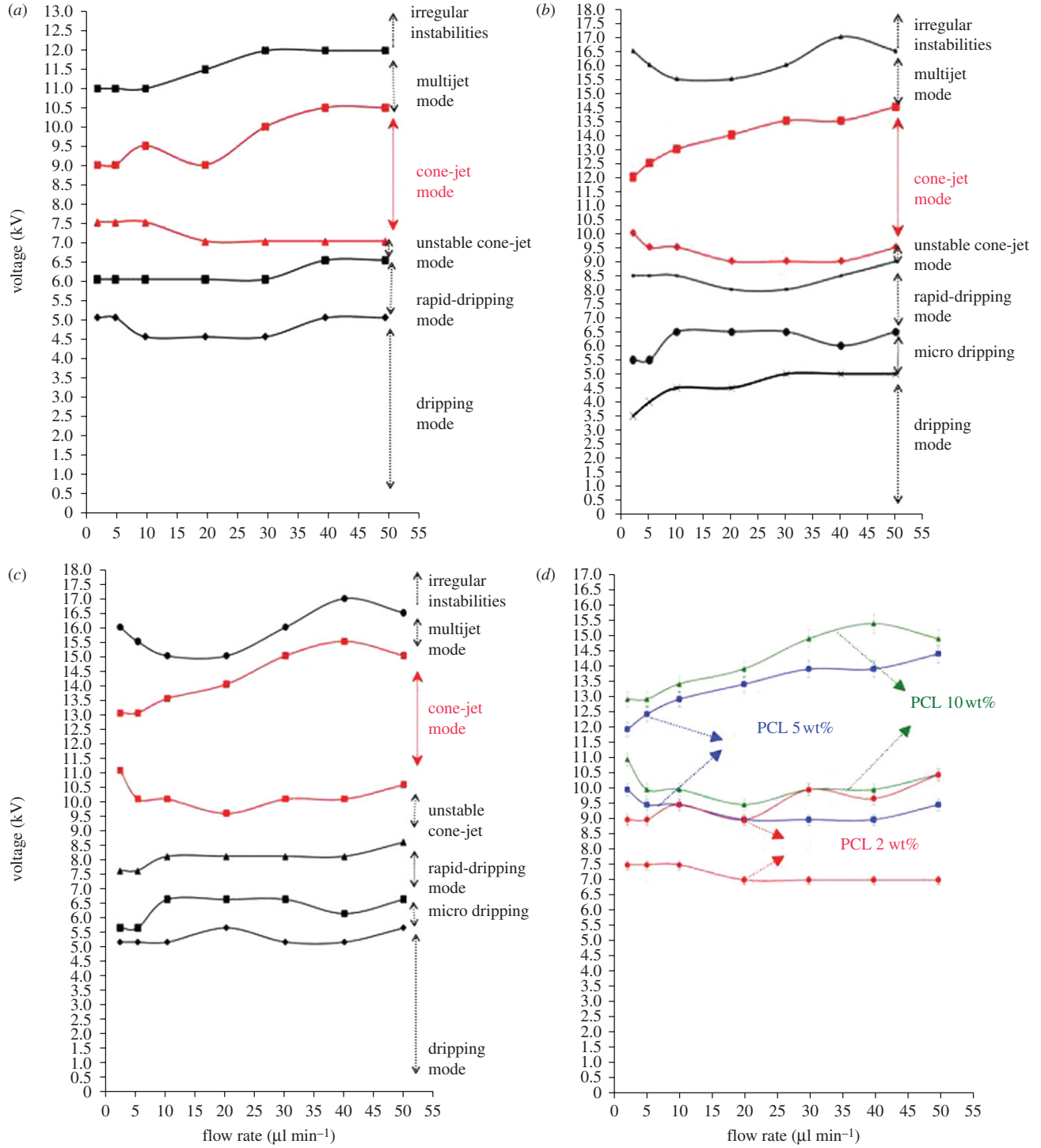

Figure 3. Operating ranges used to obtain different spraying modes (*a*) PCL : DMAC 2 : 98 (wt%), (*b*) PCL : DMAC 5 : 95 (wt%), (*c*) PCL : DMAC 10 : 90 (wt%). (*d*) Comparison of the cone-jet mode region of different solutions. (*d*) Triangles, PCL 10 wt%; circles, PCL 5 wt%; diamonds, PCL 2 wt%.

there is a considerable difference in the stability and flow of materials in real time.

These modes were investigated in detail for three different polymer concentrations and the findings are presented as parametric maps of applied voltage versus flow rate (figure 3). Mode mapping of these solutions showed that in more viscous solutions, the upper and lower limits of the voltage required for forming the stable cone-jet increased. For instance, at a flow rate of 2 µl min^{-1}, the lower limit of the applied voltage for the least viscous solution (2.6 mPa s) was 7.5 kV, whereas that for the most viscous solution (11.1 mPa s) was 11 kV (figure 3*d*). This is mainly because of the lower conductivity of the more viscous solutions. Therefore, a stronger and dominant tangential electric field should be applied to overcome the surface tension and liquid viscosity to form a cone-jet (Li & Yin 2006; Pancholi *et al.* 2009). In less viscous solutions, the regions for different jetting modes occupied a smaller area on the parametric map and transition between

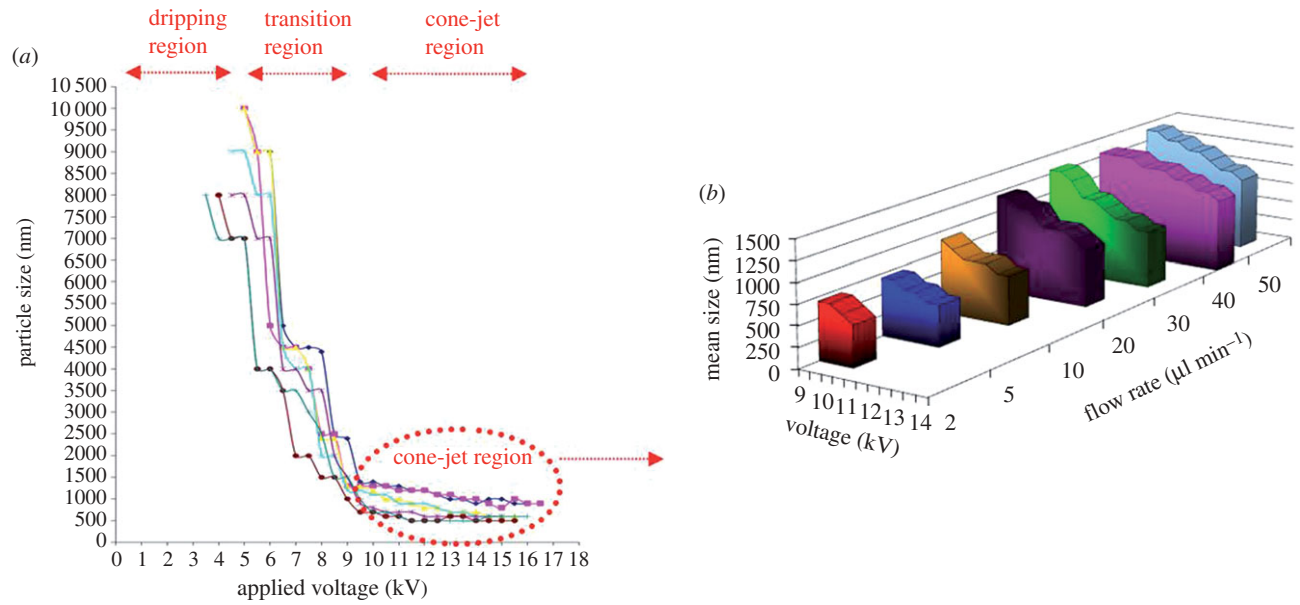

Figure 4. Variation of mean size of the particles obtained as (*a*) a function of applied voltage and flow rate and (*b*) highlighting the cone-jet region for PCL : DMAC 5 : 95 wt% solution. (*a*) Blue diamond line, F.R. = 50 µl min^{-1}; pink square line, F.R. = 40 µl min^{-1}; yellow line, F.R. = 30 µl min^{-1}; dark blue line, F.R. = 20 µl min^{-1}; pink cross line, 10 µl min^{-1}; red diamond line, 5 µl min^{-1}; green line, 2 µl min^{-1}; (*b*) blue bar, 50 µl min^{-1}; pink bar, 40 µl min^{-1}; green bar, 30 µl min^{-1}; purple bar, 20 µl min^{-1}; brown bar, 10 µl min^{-1}; dark blue bar, 5 µl min^{-1}; red bar, 2 µl min^{-1}.

modes occurred more quickly as the applied voltage increased (figure 3*a*–*c*). The difference between the lower and the upper limits of the cone-jet mode increased with an increase in the flow rate, and this could be owing to the presence of a greater volume of liquid that maintains the balance between the surface tension and electrical forces. Also, the electrical stresses could be more efficiently transmitted throughout the bulk liquid by viscous diffusion at higher flow rates.

3.3. Effect of applied voltage and flow rate

The effect of the applied voltage and flow rate on the mean size of the particles is shown in figure 4*a*. Prior to the attainment of the stable cone-jet region, the reduction in droplet size was enhanced by increasing the voltage as the mode of jetting changed from dripping to unstable cone-jet. The droplet size electrosprayed from the stable-cone was also found to decrease as the applied voltage increased, but this phenomenon was more noticeable at higher flow rates, for instance the mean size of particles produced from PCL 5 wt% decreased from 700 to 500 nm at 2 µl min^{-1} flow rate as the voltage increased (from 10 to 12 kV), whereas at 50 µl min^{-1} flow rate, the mean size reduced from 1400 to 900 nm (figure 4*b*). This is because at a lower flow rate, insufficient solution was available to affect the electrohydrodynamic forces on the droplet (Pancholi *et al.* 2008), thus, the appropriate range of applied voltage for forming the cone-jet was narrow. The voltage difference between the upper and the lower limits was less at lower flow rates, which also results in a reduction of particle size. As a result, the influence of applied voltage on particle size was relatively insignificant at a low flow rate (e.g. 2 µl min^{-1}) in the cone-jet region. Based on a method proposed by Farook *et al.* (2009), a theoretical yield of 10^{18} particles min^{-1}

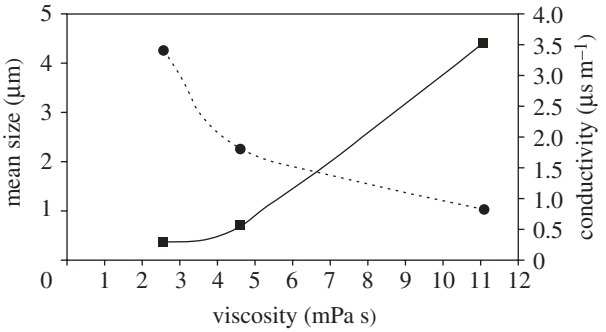

Figure 5. Relationship between mean particle size generated and the electrical conductivity and the viscosity of the PCL solutions used (flow rate: 10 µl min^{-1}, applied voltage: 10 kV). Square with solid line, mean size; circle with dotted line, conductivity.

is achievable for the production of particles with a mean size of 310 nm with a single needle. The process is also amenable to being scaled-up using multiple needle sets.

The ability to change particle size in this systematic way is of crucial significance in biotechnology as there are several size-dependent particle transport processes in the human body. Particles can pass through biological barriers by a number of different methods. These include passive (diffusive) and active processes ranging from extravasation to transdermal uptake. Most of these processes affect distribution and clearance of micro- and nano-particles in the human body and they strongly depend on particle size (Kohane 2007; Singh *et al.* 2007).

3.4. Effect of viscosity on size

Droplet diameter is greatly influenced by solution viscosity (Jayasinghe & Edirisinghe 2002). The mean

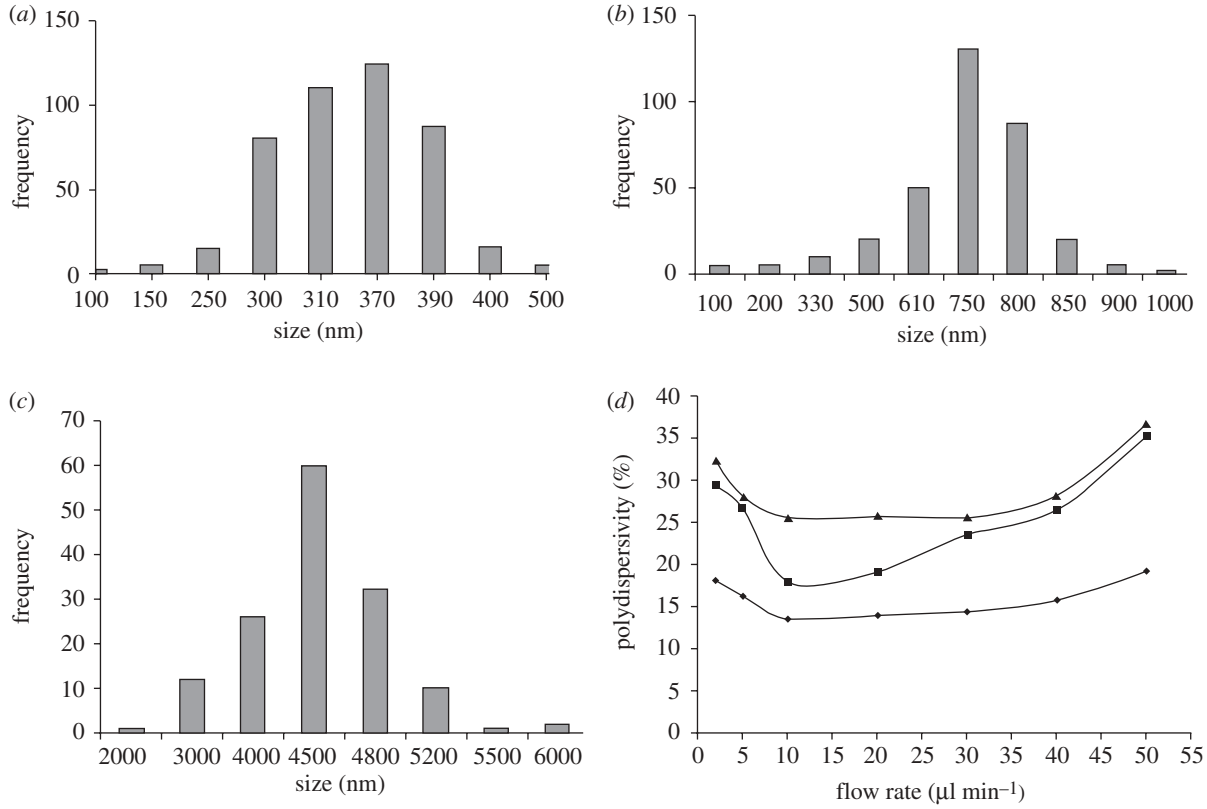

Figure 6. Size distribution of PCL particles produced using different concentrations of PCL solution (*a*) PCL 2 wt%, (*b*) PCL 5 wt%, (*c*) PCL 10 wt%, (flow rate: 10 μl min^{-1}, applied voltage: 10 kV), (*d*) polydispersivity index of particles produced in the cone-jet region as a function of flow rate (applied voltage: 10 kV). (*d*) Square line, PCL 2 wt% (viscosity: 2.6 mPa s); triangle line, PCL 5 wt% (viscosity: 4.6 mPa s); diamond line, PCL 10 wt% (viscosity: 11.1 mPa s).

size of particles obtained for solutions with different viscosities is shown in figure 5. As the concentration of PCL is varied from 2 to 10 wt%, the viscosity and the electrical conductivity of the PCL solutions changed from 2.6 to 11 (mPa s) and from 3.4 to 0.8 (μs m^{-1}), respectively. This also results in a mean particle size increase from 300 to 4500 nm. This is because of the local shear viscosity increasing and resulting in the formation of larger droplets under the action of electrohydrodynamic forces (Jaworek & Krupa 1999). The particle size distributions are shown in figure 6. All the samples displayed monomodal size distributions, however particles made from the more viscous solutions generated a narrower size distribution. Further investigation was carried out to find out the impact of viscosity and flow rate on the polydispersivity of the samples. It was observed that the polydispersivity index (standard deviation/mean) increased at the upper limit and the lower limit of flow rate in the stable cone-jet region and this influence was more noticeable at lower viscosities (figure 6*d*). This may be attributed to the stability of the cone-jet, which can dictate the size distribution of the generated morphologies. At the lower limit of flow rate within the cone-jet region, the polydispersivity was high and this correlates with slight changes to the cone-jet structure. At reduced flow rates, the apex of the cone shifts away from the centre of the cone, which is no longer symmetrical and takes the form of an 'off-centred' jet, which may alter the balance of interacting forces. However, with the increase of the flow rate, the charge on the liquid jet increases, and the repulsion force owing to the electric charge competes with the surface tension of the liquid. With much higher surface charge, the repulsion force of the charge becomes stronger, resulting in jet oscillation that produces satellites droplets (Hartman *et al.* 2000). Therefore, the number of satellite droplets and secondary droplets depend on the liquid flow rate and their quantity will increase at higher flow rates, which in turn results in a higher polydispersivity index.

3.5. *Effect of drug loading on size and morphology*

The particle size and size distribution have implications for a number of biomedical applications as explained in §1, thus studying its effect on size and morphology of the structures is crucial. In this part of the study, β-oestradiol drug, which is a sex hormone and also the most potent naturally occurring oestrogen in mammals, was incorporated in the PCL particles to assess drug release. β-Oestradiol also has therapeutic use as a contraceptive and hypocholesteraemic drug, and it has been found that β-oestradiol intake may decrease the risk of Alzheimer's disease by promoting the growth and survival of cholinergic neurons and reducing cerebral amyloid deposition (Al-Ghananeem *et al.* 2002; Bodor & Buchwald 2002; Yoo & Lee 2006).

SEM and optical microscopy images of the 'blank' particles obtained at different PCL concentrations are presented in figure 7. It was observed that particles

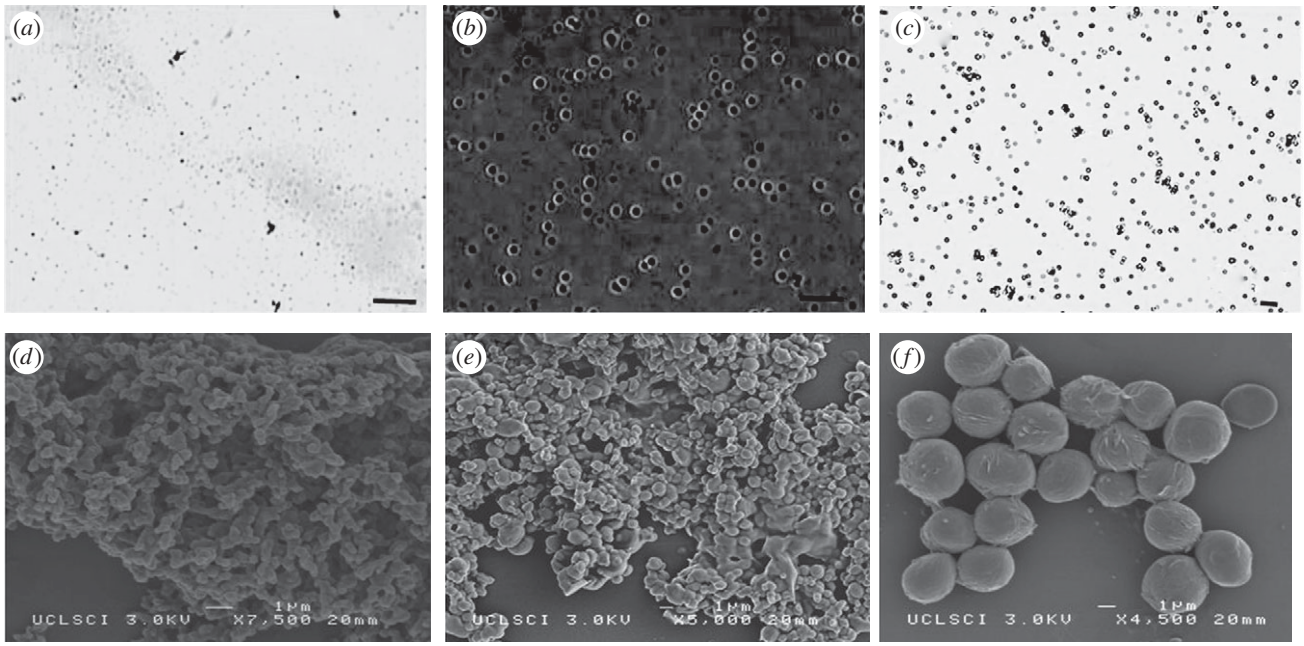

Figure 7. (*a–c*) Optical micrographs and (*d–f*) SEM images of particles prepared at different polymer concentrations. ((*a*) 2 wt% PCL, (*b*) 5 wt% PCL, and (*c*) 10 wt% PCL), flow rate = 10 μl min^{-1}, collecting distance = 150 mm, voltage approximately 10 kV. Scale bars, (*a*,*b*) 3 μm; (*c*) 20 μm.

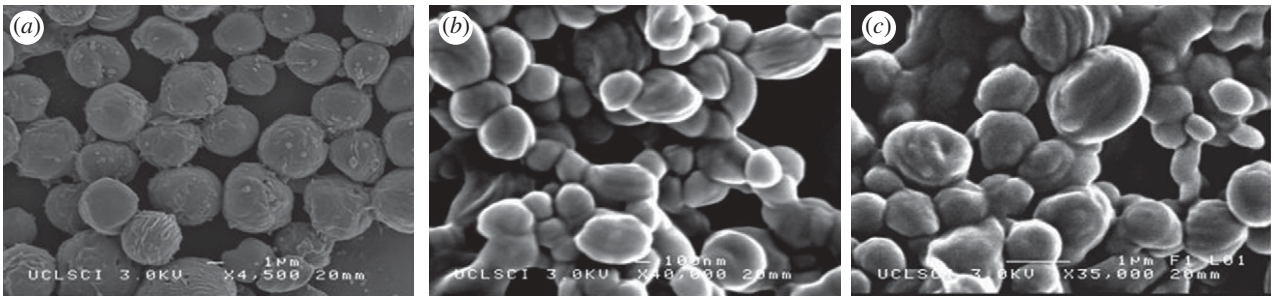

Figure 8. Scanning electron micrographs of PCL particles incorporating β-oestradiol. (*a*) 10 wt% PCL, (*b*) 5 wt% PCL, and (*c*) 2 wt% PCL with each contains 15 wt% β-oestradiol, flow rate = 10 μl min^{-1}, collecting distance = 150 mm, voltage approximately 10 kV.

were round in shape with a relatively smooth surface. Particles produced from less concentrated solutions (lower viscosity) were more aggregated to each other which could be owing to the presence of solvent soon after particle collection. Changes in the morphology and structure of the resulting particles were also studied (figure 8). The mean size of the particles was calculated by measuring the diameter of approximately 400 particles using the UTHSCSA imaging tool program. It was observed that the morphology of the particles didn't change noticeably, but a small increase of 5–13% in the mean size of the particles was observed (table 2). This increase in size may be attributed to swelling due to the entrapment of drug in the particles.

3.6. In vitro *release study*

The degradation of PCL is significantly slower than that of other extensively investigated polymers and copolymers, such as lactic and glycolic acids and is therefore suitable for the design of long-term drug-delivery systems (Engelberg & Kohn 1991). Release of drugs from polymeric particles in which the drug particles are dispersed in the polymer matrix occurs by the permeation of solvent through the polymer matrix to the drug molecules, dissolution of the drug particle and diffusion of the drug through the polymer to the release medium (Spenlehauer *et al.* 1988).

The drug-release profiles for particles with the size range of 340–4600 nm obtained using UV spectrophotometry are shown in figure 9. The encapsulation efficiencies of the particles made from 2, 5 and 10 wt% PCL solutions were 85 per cent, 88 per cent and 89 per cent, respectively. Drug-loaded PCL particles showed sustained release of β-oestradiol. An initial rapid release period from the particles was observed in all samples. This was thought to be due to dissolution/diffusion of β-oestradiol from the superficial regions of the particles, an effect that has been documented for the release of many drugs from polymeric microspheres (Spenlehauer *et al.* 1988). Generally, drug release from PCL particles owing to degradation or erosion of the polymer is thought to be unlikely because previous studies show no significant

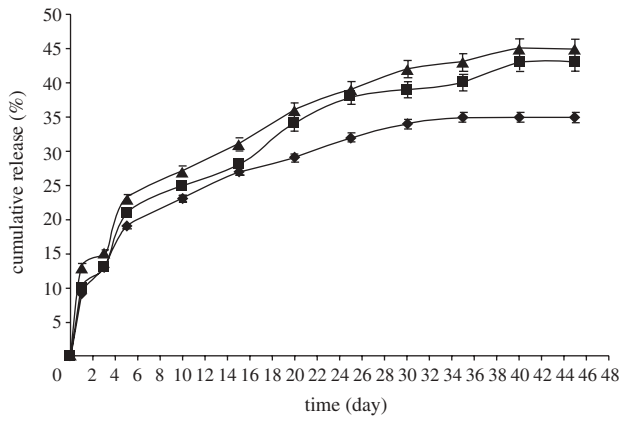

Figure 9. β-oestradiol release profile of PCL particles prepared from different PCL solutions loaded with 15 wt% β-oestradiol. Diamond line, PCL 10 wt%; square line, PCL 5 wt%; triangle line, PCL 2 wt%.

Table 2. Size of 'blank' and drug-loaded particles at various polymer concentrations.

sample	mean size of the blank particles μm^{-1}	mean size of the particles loaded with 15 wt% β-oestradiol μm^{-1}
PCL : DMAC 2 : 98	0.31	0.34
PCL : DMAC 5 : 95	0.71	0.8
PCL : DMAC 10 : 90	4.4	4.6

weight loss or surface erosion of PCL over a seven-week period (Sefton *et al.* 1984; Izumikawa *et al.* 1991). After the initial release phase of 6 days, 36, 42 and 45 per cent of the loaded drug was released from samples prepared from PCL 10 wt%, PCL 5 wt% and PCL 2 wt%, respectively, at a slower release rate. This could be explained by the fact that the particles fabricated with the dilute solution had a smaller size and with a decrease in particle size, the surface area to volume ratio increases leading to increased SBF penetration and faster escape of the drug.

4. CONCLUSIONS

A method of particle production providing systematic variation of size and size distribution has been demonstrated at ambient temperature and pressure, with easily adjustable applied voltage and flow rate serving as process control parameters. The range of operating parameters in terms of flow rate, applied voltage and the inherent properties of solutions such as viscosity and electrical conductivity were identified for the ideal processing window of stable jetting (cone-jet). It was found that in more viscous solutions, the upper and the lower limits of the required voltage for forming the stable cone-jet increased from 7.5 to 11 kV. The size of the particles obtained within the stable cone-jet mode window was found to decrease as the applied voltage increased, but this phenomenon was more noticeable at higher flow rates. Particle diameter was also greatly influenced by liquid viscosity, the mean size of particles changed from 340 to 4400 nm as the viscosity increased from 2.5 to 11 mPa s. The size distribution of all samples was monomodal but it was found that the polydispersivity index of the particles increased at the upper limit and the lower limit of flow rates in the cone-jet region. It was observed that loading 15 wt% β-oestradiol as a model drug to the PCL solutions changed the electrical conductivity of the solutions and increased the size of the particles, but did not have a significant impact on the morphology of the particles. The *in vitro* release study showed a sustained release profile from PCL particles over 45 days with a maximum EE of 89 per cent at 10 wt% PCL.

The authors thank the EPSRC and the Royal Academy of Engineering for supporting this work through Prof. Edirisinghe's platform grant (EP/E045839) and Dr Stride's Research Fellowship and also UCL for supporting Ms Enayati via an Overseas Research Scholarship.

REFERENCES

Aberturas, M. R., Molpeceres, J., Guzman, M. & Garcia, F. 2002 Development of a new cyclosporine formulation based on poly (caprolactone) microspheres. *J. Microencapsul.* **19**, 61–72. (doi:10.1080/02652040110055270)

Ahmad, Z., Zhang, H. B., Farook, U., Edirisinghe, M., Stride, E. & Colombo, P. 2008 Generation of multilayered structures for biomedical applications using a novel tri-needle coaxial device and electrohydrodynamic flow. *J. R. Soc. Interface* **27**, 1255–1261. (doi:10.1098/rsif.2008.0247)

Al-Ghananeem, A. M., Traboulsi, A. A., Dittert, L. W. & Hussain, A. A. 2002 Targeted brain delivery of 17β-estradiol via nasally administered water soluble prodrugs. *AAPS PharmSciTech* **3**, 1–8. (doi:10.1208/pt030105)

Bodor, N. & Buchwald, P. 2002 Barriers to remember: brain-targeting chemical delivery systems and Alzheimer's disease. *Drug Discov. Today* **7**, 766–774. (doi:10.1016/S1359-6446(02)02332-2)

Borra, J. P., Tombette, Y. & Ehouarn, P. 1999 Influence of electric field profile and polarity on the mode of EHDA related to electric discharge regimes. *J. Aerosol Sci.* **30**, 913–925. (doi:10.1016/S0021-8502(98)00779-4)

Calvo, P. *et al.* 2001 Long-circulating PEGylated polycyanoacrylate nanoparticles as new drug carrier for brain delivery. *Pharm. Res.* **18**, 1157–1166. (doi:10.1023/A:1010931127745)

Chowdary, K. P. & Rao, Y. S. 2004 Mucoadhesive microspheres for controlled drug delivery. *Biol. Pharm. Bull.* **27**, 1717–1724. (doi:10.1248/bpb.27.1717)

Cloupeau, M. & Prunet-Foch, B. 1990 Electrostatic spraying of liquids: main functioning modes. *J. Electrostat.* **25**, 165–184. (doi:10.1016/0304-3886(90)90025-Q)

Edwards, D. A. *et al.* 1997 Large porous particles for pulmonary drug delivery. *Science* **276**, 1868–1871. (doi:10.1126/science.276.5320.1868)

Enayati, M., Ahmad, Z., Stride, E. & Edirisinghe, M. 2009 Preparation of polymeric carriers for drug delivery with different shape and size using an electric jet. *Curr. Pharm. Biotechnol.* **10**, 600–608. (doi:10.2174/138920109789069323)

Enayati, M., Ahmad, Z., Stride, E. & Edirisinghe, M. 2010 One-step electrohydrodynamic production of drug-loaded micro- and nanoparticles. *J. R. Soc. Interface* **7**, 667–675. (doi:10.1098/rsif.2009.0348)

Engelberg, I. & Kohn, J. 1991 Physico-mechanical properties of degradable polymers used in medical applications. *Biomaterials* **12**, 292–304. (doi:10.1016/0142-9612(91)90037-B)

Farook, U., Stride, E. & Edirisinghe, M. J. 2009 Preparation of suspensions of phospholipid-coated microbubbles by coaxial electrohydrodynamic atomization. *J. R. Soc. Interface* **6**, 271–277. (doi:10.1098/rsif.2008.0225)

Hartman, R. P. A., Brunner, D. J., Camelot, D. M. A., Marijnissen, J. C. M. & Scarlett, B. 1999 Electrohydrodynamic atomization in the cone-jet mode physical modeling of the liquid cone and jet. *J. Aerosol Sci.* **30**, 823–849. (doi:10.1016/S0021-8502(97)85263-9)

Hartman, R. P. A., Brunner, D. J., Camelot, D. M. A., Marijnissen, J. C. M. & Scarlett, B. 2000 Jet break-up in electrohydrodynamic atomization in the cone-jet mode. *J. Aerosol Sci.* **31**, 65–95. (doi:10.1016/S0021-8502(99)00034-8)

Izumikawa, S., Yoshioka, S., Aso, Y. & Takeda, Y. 1991 Preparation of poly(l-lactide) microspheres of different crystalline morphology and effect of crystalline morphology on drug release rate. *J. Control. Release* **15**, 133–140. (doi:10.1016/0168-3659(91)90071-K)

Jaworek, A. & Krupa, A. 1999 Jet and drops formation in electrhydrodynamic spraying of liquids. A system approach. *Exp. Fluids* **27**, 43–52. (doi:10.1007/s003480050327)

Jayasinghe, S. N. & Edirisinghe, M. J. 2002 Effect of viscosity on the size of relics produced by electrostatic atomization. *J. Aerosol. Sci.* **33**, 1379–1388. (doi:10.1016/S0021-8502(02)00088-5)

Kaul, G. & Amiji, M. 2005 Tumor-targeted gene delivery using poly(ethylene glycol)-modified gelatin nanoparticles: *in vitro* and *in vivo* studies. *Pharm. Res.* **22**, 951–961. (doi:10.1007/s11095-005-4590-3)

Kohane, D. S. 2007 Microparticles and nanoparticles for drug delivery. *Biotechnol. Bioeng.* **96**, 203–209. (doi:10.1002/bit.21301)

Lanza, G. M. *et al.* 2002 Targeted antiproliferative drug delivery to vascular smooth muscle cells with a magnetic resonance imaging nanoparticle contrast agent: implications for rational therapy of restenosis. *Circulation* **106**, 2842–2847. (doi:10.1161/01.CIR.0000044020.27990.32)

Li, F. & Yin, X. Y. 2006 Linear instability of a co-flowing jet under an axial electric field.. *Phys. Rev. E* **74**, 036 304–036 307. (doi:10.1103/PhysRevE.74.036304)

Mitragotri, S. & Lahann, J. 2009 Physical approaches to biomaterial design. *Nat. Mater.* **8**, 15–23. (doi:10.1038/nmat2344)

Monsky, W. L., Fukumura, D., Gohongi, T., Ancukiewcz, M., Weich, H. A., Torchilin, V. P., Yuan, F. & Jain, R. K. 1999 Augmentation of transvascular transport of macromolecules and nanoparticles in tumors using vascular endothelial growth factor. *Cancer Res.* **59**, 4129–4135.

Musante, C. J., Schroeter, J. D., Rosati, J. A., Crowder, T. M., Hickey, A. J. & Martonen, T. B. 2002 Factors affecting the deposition of inhaled porous drug particles. *J. Pharm. Sci.* **91**, 1590–1600. (doi:10.1002/jps.10152)

Oyewumi, M. O. & Mumper, R. J. 2003 Influence of formulation parameters on gadolinium entrapment and tumor cell uptake using folate-coated nanoparticles. *Int. J. Pharm.* **251**, 85–97. (doi:10.1016/S0378-5173(02)00587-2)

Pancholi, K. P., Stride, E. & Edirisinghe, M. 2008 Generation of microbubbles for diagnostic and therapeutic applications using a novel device. *J. Drug Target* **16**, 494–501. (doi:10.1080/10611860802184884)

Pancholi, K. P., Ahras, N., Stride, E. & Edirisinghe, M. 2009 Novel electrohydrodynamic preparation of porous chitosan particles for drug delivery. *J. Mater. Sci. Mater. Med.* **20**, 917–923. (doi:10.1007/s10856-008-3638-4)

Panyam, J. & Labhasetwar, V. 2003 Biodegradable nanoparticles for drug and gene delivery to cells and tissue. *Adv. Drug Deliv. Rev.* **55**, 329–347. (doi:10.1016/S0169-409X(02)00228-4)

Reed, A. M. & Gilding, D. K. 1981 Biodegradable polymers for use in surgery—poly(glycolic)-poly(lactic acid) homo and co-polymers.2. *In vitro* Degradation. *Polymer* **22**, 494–498. (doi:10.1016/0032-3861(79)90009-0)

Sefton, M. V., Brown, L. R. & Langer, R. S. 1984 Ethylene-vinyl acetate copolymer microspheres for controlled release of macromolecules. *J. Pharm. Sci.* **71**, 1859–1861. (doi:10.1002/jps.2600731258)

Shive, M. S. & Anderson, J. M. 1997 Biodegradation and biocompatibility of PLA and PLGA microspheres. *Adv. Drug Deliv. Rev* **28**, 5–24. (doi:10.1016/S0169-409X(97)00048-3)

Singh, M., Chakrapani, A. & O'Hagan, D. 2007 Nanoparticles and microparticles as vaccine-delivery systems. *Expert Rev. Vaccines* **6**, 797–808. (doi:10.1586/14760584.6.5.797)

Song, C., Labhasetwar, V., Cui, X., Underwood, T. & Levy, R. J. 1998 Arterial uptake of biodegradable nanoparticles for intravascular local drug delivery: results with an acute dog model. *J Control. Release* **54**, 201–211. (doi:10.1016/S0168-3659(98)00016-9)

Spenlehauer, G., Vert, M., Benoit, J. P., Chabot, F. & Veillard, M. 1988 Biodegradable cisplatin microspheres prepared by the solvent evaporation method: morphology and release characteristics. *J Control. Release* **7**, 217–229. (doi:10.1016/0168-3659(88)90054-5)

Stroh, M. *et al.* 2005 Quantum dots spectrally distinguish multiple species within the tumor milieu *in vivo*. *Nat. Med.* **11**, 678–682. (doi:10.1038/nm1247)

Valo, H., Peltonen, L., Vehvilainen, S., Karjalainen, M., Kostiainen, R., Laaksonen, T. & Hirvonen, J. 2009 Electrospray encapsulation of hydrophilic and hydrophobic drugs in poly(L-lactic acid) nanoparticles. *Small* **5**, 1791–1798. (doi:10.1002/smll.200801907)

Wang, K. & Stark, J. P. W. 2010 Deposition of colloidal gold nanoparticles by fully pulsed-voltage-controlled electrohydrodynamic atomisation. *J. Nanopart. Res.* **12**, 707–711. (doi:10.1007/s11051-009-9825-5)

Wu, Y., MacKay, J. A., McDaniel, J. R., Chilkoti, A. & Clark, R. L. 2009 Fabrication of elastin-like polypeptide nanoparticles for drug delivery by electrospraying. *Biomacromolecules* **10**, 19–24. (doi:10.1021/bm801033f)

Xie, J., Lim, L. K., Phua, Y., Hua, J. & Wang, C. H. 2006 Electrohydrodynamic atomization for biodegradable polymeric particle production. *J. Colloid Interface Sci.* **302**, 103–112. (doi:10.1016/j.jcis.2006.06.037)

Yoo, J. W. & Lee, C. H. 2006 Drug delivery systems for hormone therapy. *J. Control. Release* **112**, 1–14. (doi:10.1016/j.jconrel.2006.01.021)